Patterned femtosecond laser excitation of terahertz leaky modes in GaAs photonic crystals

Nathan Jukam,[a] Cristo Yee, and Mark S. Sherwin
Department of Physics, University of California, Santa Barbara, California 93106

Ilya Fushman and Jelena Vučković
Department of Electrical Engineering, Stanford University, Stanford, California, 94305

(Received 5 July 2006; accepted 22 October 2006; published online 13 December 2006)

GaAs terahertz (THz) photonic crystals are fabricated using reactive ion etching. A femtosecond laser beam generates THz radiation inside the PCs. Spatial patterning of the laser beam is used to couple into the PC modes. THz emission is observed from modes above the light line (leaky modes). Only the dipole modes are found to radiate strongly in the direction normal to the slab which is consistent with finite-difference time-domain based calculations of the far fields. © *2006 American Institute of Physics*. [DOI: 10.1063/1.2399439]

Photonic crystals (PCs) allow the engineering of the optical properties of materials.[1] PCs in the terahertz (THz) frequency spectrum are of interest, as they could contribute toward improving THz technology. In contrast to passive Si,[2,3] metallic,[4] and polyethylene[5] THz PCs, one can envision active devices (such as THz quantum cascade lasers[6]) embedded in a THz GaAs PC.

PCs may possess photonic band gaps where light of a given frequency cannot propagate. By introducing defects in a PC with a band gap, resonant cavities can be formed. Such cavities can enhance the spontaneous emission rate and create low threshold lasers.[7]

Quasi resonators can also be formed from PC modes that have wave vectors at high symmetry points of the Brillouin zone. Modes at these points have a high photonic density of states and low group velocities which can lead to gain enhancement.[8]

A PC slab is a two-dimensional PC with a thickness on the order of a wavelength. The leaky modes of a PC slab lie above the light line, as shown in Fig. 1(a). In contrast to guided modes, which lie below the light line, leaky modes can be diffracted out of the PC slab into free space.[9] Lasing from PC leaky modes at high symmetry points has been achieved,[10] and demonstrations include lasing from a quantum cascade structure.[11]

In this letter THz PC slabs are fabricated out of GaAs and their leaky mode resonances are investigated. THz radiation is created inside the GaAs PC slab using a femtosecond laser. THz field patterns with length scales less than THz wavelengths are created in the PC slab by spatially patterning the femtosecond laser beam. This allows THz radiation to be directly coupled into the PC's modes. Emission of leaky modes out of the slab via diffraction is observed using free space electro-optic (EO) sampling.[12]

THz PCs were fabricated using reactive ion etching in an inductively coupled plasma. Air holes were etched in a semi-insulating $\langle 100 \rangle$ 500 μm thick GaAs wafer to a target depth of 60 μm.[13] The air holes were arranged in a triangular lattice with a lattice constant a of 150 μm [Fig. 1(b)]. To form a PC slab the wafer was flipped over and the substrate was etched to the bottom of the air holes over a 4 mm diameter[14] [Fig. 1(c)]. No etch stop was used, which caused variations in the thickness of the slabs. Sample I had an air hole radius r of $0.26a$ and a thickness d of $0.4 \pm 0.03a$. Sample II was over etched with $d=0.27 \pm 0.03a$ and $r=0.31a$.

The GaAs wafer had a 2 μm n-doped (2×10^{16} cm^{-3}) epilayer. Femtosecond laser pulses[15] created photocarriers at the GaAs surface which were accelerated by the surface depletion field. This drove plasma oscillations in the epilayer which generated THz radiation.[16]

To couple THz radiation into a PC mode, the inner product of the PC mode's electric field and the plasma-generated THz field must be nonzero.[17] To achieve this, a patterned photomask was placed in the pump beam path, and its image was projected onto the PC with a lens, as shown in Fig. 2. The emitted THz radiation was collected from the side of the PC without the doped epilayer. Free space EO sampling[12] with a $\langle 110 \rangle$ ZnTe crystal was used to measure the emitted THz radiation. EO sampling only detects the THz field component parallel to the $\langle 110 \rangle$ edge of the ZnTe crystal. The polarization of the emitted THz radiation could be investigated by rotating the ZnTe crystal by 90°. By moving only the photomask, the position of the laser pattern on the PC could be moved without disturbing the alignment of the THz radiation and femtosecond laser beams.

For an unprocessed portion of the GaAs wafer, a one cycle electromagnetic pulse with a broad spectrum was emitted [upper trace in Fig. 3(a)]. The emitted power was maximized with the wafer tilted near Brewster's angle (74°). At normal incidence no THz radiation was observed, because the plasma oscillates parallel to the laser's wave vector.[18]

With uniform laser excitation at normal incidence, no THz radiation was observed from the PCs [lower trace in

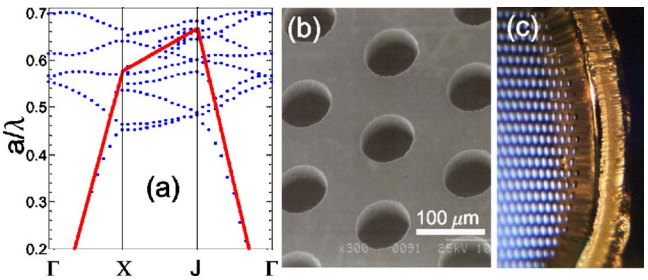

FIG. 1. (Color online) (a) Band diagram of the TM modes of a PC slab for $d=0.275$ and $r=0.31$. The light line ($\omega^2=c^2\mathbf{k}^2$) is the red line. (b) SEM picture of a PC slab. (c) Photograph of the bottom of a PC slab.

[a]Electronic mail: njukam@physics.ucsb.edu

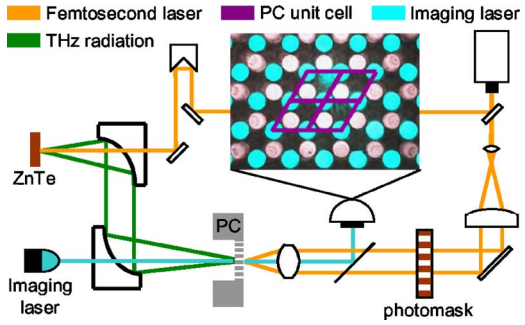

FIG. 2. The femtosecond laser beam is expanded (×4) and sent through a photomask. The image of the photomask is projected onto the sample with a 30 mm lens. A pellicle beam splitter sends the PC surface reflection into a webcam. An imaging laser illuminates the air holes. Paraboloidal mirrors collect the emitted THz radiation from the PC and refocus it into a 2 mm ZnTe crystal. The imaging laser and the EO probe beam pass through small holes drilled into the paraboloidal mirrors.

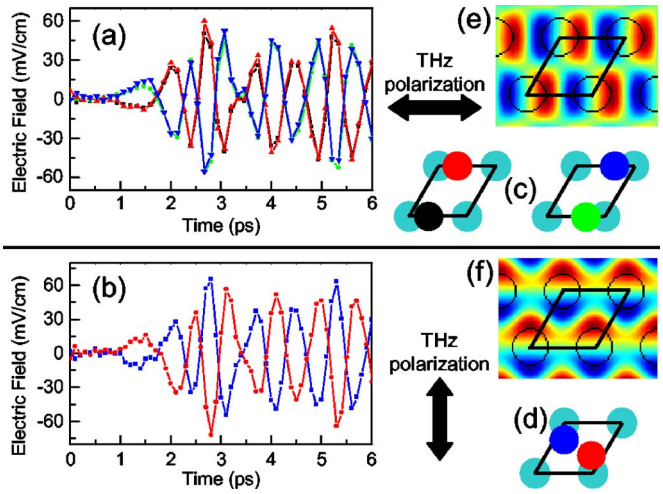

FIG. 4. Horizontal (a) and vertical (b) components of the emitted THz electric field with the triangular pattern of laser spots shown in Fig. 2. The unit cell diagrams indicate the positions of the laser pattern for horizontal (c) and vertical (d) polarizations, relative to the PC's air holes. The colored spots in (c) and (d) correspond to the positions at which the data of the same color were taken in (a) and (b). (e) and (f) show FDTD-calculated E_z fields of the degenerate dipole modes (color chart: red, positive; blue, negative).

Fig. 3(a)]. However, for the patterned laser excitation in Figs. 3(b) and 3(c), THz spectra consisting of peaks were observed from both samples. The resonances of sample II are at higher frequencies than those of sample I, since sample II has less dielectric material than sample I.[1] The broader peak of sample II is attributed to the slightly oblong shape of its air holes. The peak spectral power from the PCs is on the order of 10% of the spectral power of an unprocessed wafer tilted at Brewster's angle.

The electric field profiles of the emitting PC modes were investigated by translating the triangular laser pattern shown in Fig. 2 across the PC's unit cell. The emitting modes were concentrated near the edges of the air holes for both samples I and II. Emitted THz electric fields from sample I are shown in Figs. 4(a) and 4(b) for different positions of the laser pattern [Figs. 4(c) and 4(d)]. Emitted THz radiation is polarized horizontally (vertically) when the laser spots are translated horizontally (vertically) from the centers of the air holes. The emitted THz electric field also changes sign when the laser pattern is shifted horizontally [Fig. 4(c)] or vertically [Fig. 4(d)] between opposite edges of the air holes.

The solutions of a PC slab can be separated into TM and TE modes.[1] At the center of a PC slab a TM (TE) mode will have its electric field normal (parallel) to the PC surface. Away from the center of the slab the electric field of the TM (TE) mode will have tangential (normal) components. However, inside the PC slab the electric field will be nearly normal (parallel) for TM (TE) modes.

Plasma-generated THz radiation will couple into the TM modes since the depletion field (and hence the generated THz electric field) is normal to the GaAs surface. However, at the edges of the air holes the normal of the surface is in the plane of the slab. Photogenerated carriers created at the air hole edge within 2 μm of the vertical surface could initiate plasma oscillations that would couple THz radiation into TE modes.

To confirm that the modes are TM and not TE, a stripe laser pattern is moved across the holes, as shown in Fig. 5. If the modes are TE modes (originating only at the edge of the air holes) the emitted power is expected to remain constant when the stripes are moved over the edge of the air hole and then rapidly fall to zero when the stripes leave the edge. However, in Fig. 5(a) the power of sample I's peak at 1.2 THz increases and decreases gradually as the laser stripe is moved over the edge of the air hole.

Three-dimensional finite-difference time-domain (FDTD) calculations were used to compute the TM modes at the Γ point. The patterned laser excitation has the same period as the PC and will only couple to modes at the Γ point, where $\mathbf{k}_{\mathrm{Bloch}}=0$. Contour plots (in a plane near the surface of the slab) of the out-of-plane electric field component (E_z) are shown in Fig. 4 for degenerate horizontal [Fig. 4(e)] and vertical [Fig. 4(f)] dipole modes. When the laser pattern is moved between two regions of the dipole mode that have identical magnitudes but different signs, the emitted THz field also changes sign, as shown in Fig. 4.

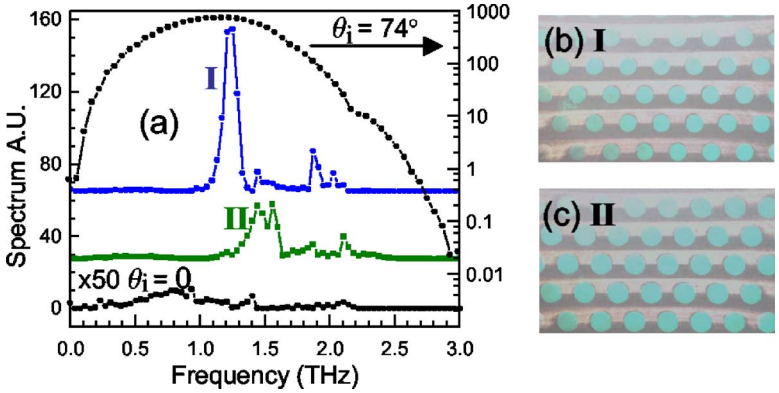

FIG. 3. (Color online) (a) Spectra of an unprocessed wafer tilted at Brewster's angle (upper trace log scale), the spectrum (×50) from sample I under uniform laser excitation (lower trace), and the spectra from samples I and II under the pattern laser excitation shown in (b) and (c), respectively.

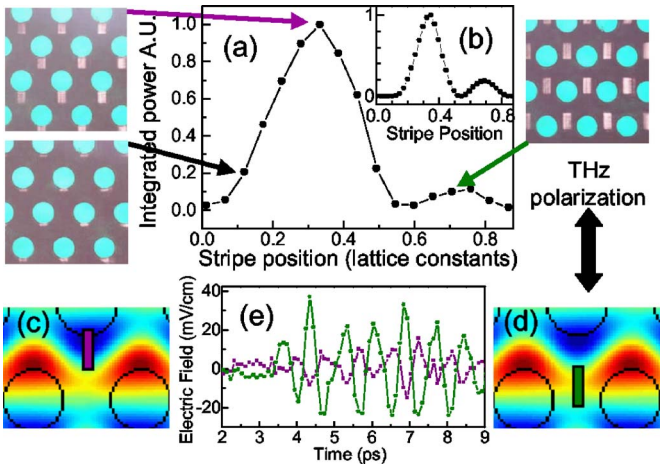

FIG. 5. (a) Integrated spectral power of the peak at 1.2 THz as a function of the position of the stripe laser pattern for sample I. (b) Calculated spectral power from the dipole mode as a function of position. [(c) and (d)] E_z component of the dipole mode showing the position of the laser stripe at the absolute maximum (c) and local maximum (d) of the integrated power in part (a). (e) electric field at the absolute maximum (purple) and local maximum (green) of the integrated power in part (a).

The FDTD-calculated frequencies of the degenerate dipole modes are 20% less than the peaks at 1.2 and 1.5 THz of samples I and II in Fig. 3(a). This could be due to a systematic error in the measurement of the slab's thickness, or the doped epilayer which is not taken into account in the FDTD calculations. The peaks near 1.9 and 2.2 THz of samples I and II are believed to be higher order slab modes (having a node in the center of the slab) of the dipole modes.

Figure 5 shows additional confirmation that the emitted THz radiation originates from the degenerate dipole modes. The power coupled into the vertical dipole mode as a function of the laser stripe position is found using FDTD calculations of the mode in Fig. 5(b). Both Figs. 5(a) and 5(b) have an absolute maximum when the laser stripe is positioned near the air hole edge and a local maximum when the laser stripe is positioned away from the air hole. The position of the laser stripe at the absolute [local] maximum is shown in Fig. 5(c) [Fig. 5(d)]. The computed electric fields (E_z) at the positions shown in Figs. 5(c) and 5(d) have opposite signs. The measured THz electric fields at the positions shown in Figs. 5(c) and 5(d) also have opposite signs, as shown in Fig. 5(e).

Near the frequency of the degenerate dipole modes the FDTD calculations also show the existence of a hexapole, a pair of degenerate quadrupoles, and a monopole. These modes are not observed experimentally. The far-field patterns of all the modes were investigated using the surface equivalence theorem.[19] The far-field radiation pattern from the PC can be calculated, if the near-field tangential fields are known in a plane above the slab. In the Fraunhofer limit the far field can be found by taking the Fourier transforms of the tangential fields. The fourier space consists of the k_x and k_y components of the emitted wave vectors. The k_z component of the emitted wave vector can be found from the free space dispersion $\omega^2=c^2\mathbf{k}^2$ where k_z may be imaginary. The point at $k_x=k_y=0$ corresponds to emission of radiation in the direction normal to the PC slab. Other points in Fourier space will correspond to either angled or evanescent emission. In Fig. 6 the tangential field components in a plane above the PC slab of the vertical degenerate dipole mode and a degenerate quadrupole mode are shown along with their corresponding Fourier transforms. The dipole mode has a strong $k_x=k_y=0$ component for the E_y and B_x fields. The quadrupole mode has no $k_x=k_y=0$ component. The hexapole, quadrupole, and monopole modes are all found to lack a $k_x=k_y=0$ component and will not radiate in the forward direction normal to the slab.

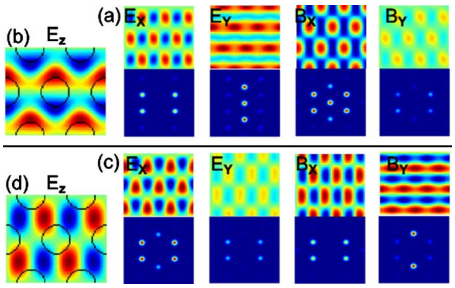

FIG. 6. (Color online) (a) Tangential fields of the vertical dipole mode in a plane above the PC slab with their apodized Fourier transforms. (b) E_z field of the vertical dipole mode in the PC slab. (c) Tangential fields and Fourier transforms of a quadrupole mode in a plane above the PC slab. (d) E_z field of the quadrupole mode in the PC slab.

The dipole modes are also the only modes with their field antinodes near the air hole edge. Alternatively, the air-dielectric interface of the air hole edge can be thought of as strongly scattering modes out of the PC slab when there is an appreciable field at the air hole edge.

The authors acknowledge support from NSF Grant No. DMR0244390.

[1] J. D. Joannopoulos, R. D. Meade, and J. N. Winn, *Photonic Crystals* (Princeton University Press, Princeton, 1995).
[2] N. Jukam and M. S. Sherwin, Appl. Phys. Lett. **83**, 21 (2003).
[3] Z. Jian, J. Pearce, and D. Mittleman, Semicond. Sci. Technol. **20**, S300 (2005).
[4] A. Bingham, Y. Zhao, and D. Grischkowsky, Appl. Phys. Lett. **87**, 051101 (2005).
[5] H. Han, H. Park, and J. Kim, Appl. Phys. Lett. **80**, 2634 (2002).
[6] R. Kohler, A. Tredicucci, F. Beltram, H. Beere, E. Linfield, A. Davies, D. Ritchie, R. Iotti, and F. Rossi, Nature (London) **417**, 156 (2002).
[7] M. Loncar, T. Yoshie, A. Scherer, P. Gogna, and Y. Qiu, Appl. Phys. Lett. **81**, 2680 (2002).
[8] J. P. Dowling, M. Scalora, M. J. Bloemer, and C. M. Bowden, J. Appl. Phys. **74**, 7 (1994).
[9] M. Boroditsky, T. F. Krauss, R. Coccioli, R. Bhat, and E. Yablonovitch, Appl. Phys. Lett. **75**, 1036 (1999).
[10] M. Meier, A. Mekis, A. Dodabalapu, A. Timko, and R. Slusher, Appl. Phys. Lett. **74**, 7 (1999).
[11] R. Colombelli, K. Srinivasan, M. Troccoli, O. Painter, C. Gmachl, and F. Capasso, Science **302**, 1374 (2003).
[12] Q. Wu and X. C. Zhang, Appl. Phys. Lett. **68**, 1604 (1996).
[13] Etch parameters were 40 SCCM BCl_3, 100 SCCM Cl_2, 20 SCCM Ar, rf bias of 100 W, inductively coupled plasma bias of 900 W, and 7 Pa. AZ960 resist was used as a mask.
[14] The slab was etched in a Panasonic E640 with identical etch parameters as the air hole etch with a 4 μm thick SiO_2 mask.
[15] A mode locked Ti:sapphire laser produced 8 nJ, 110 fs laser pulses at a central wavelength of 792 nm with a repetition rate of 82 MHz.
[16] R. Kersting, J. N. Heyman, G. Strasser, and K. Unterrainer, Phys. Rev. Lett. **79**, 3038 (1997); Phys. Rev. B **58**, 4533 (1998).
[17] Any arbitrary electric field in the PC can be represented as the sum of orthogonal PC modes. The inner product is the dot product of the plasma-generated THz field and the field of the PC mode integrated over a unit cell.
[18] M. B. Jonston, D. M. Whittaker, A. Corchia, A. G. Davies, and E. H. Linfield, Phys. Rev. B **66**, 165301 (2001).
[19] J. Vučković, H. Mabuchi, M. Loncar, and A. Scherer, IEEE J. Quantum Electron. **38**, 850 (2002).